PHOTOSYNTHETICA
International Journal for Photosynthesis Research

DOI 10.32615/ps.2023.033 PHOTOSYNTHETICA 61 (SI): 432-440, 2023

Special issue in honor of Prof. Győző Garab

Priming of *Pisum sativum* seeds with stabilized *Pluronic P85* nanomicelles: effects on seedling development and photosynthetic function

S. KRUMOVA[*], A. PETROVA[**], D. KOLEVA[***], S. PETROVA[*], S. STOICHEV[*], N. PETROVA[*,#], T. TSONEV[*], P. PETROV[##], and V. VELIKOVA[*,**,+]

Institute of Biophysics and Biomedical Engineering, Bulgarian Academy of Sciences, Sofia, Bulgaria[*]
Institute of Plant Physiology and Genetics, Bulgarian Academy of Sciences, Sofia, Bulgaria[**]
Faculty of Biology, Sofia University 'St. Kliment Ohridsky', Sofia, Bulgaria[***]
Institute of Plant Biology, Biological Research Centre, Szeged, Hungary[#]
Institute of Polymers, Bulgarian Academy of Sciences, Sofia, Bulgaria[##]

Abstract

Natural and synthetic polymers are widely explored for improving seed germination and plant resistance to environmental constraints. Here, for the first time, we explore stabilized nanomicelles composed of the biocompatible triblock co-polymer *Pluronic P85* (SPM) as a priming agent for *Pisum sativum* (var. RAN-1) seeds. We tested a wide concentration range of 0.04–30 g(SPM) L^{-1}. Applying several structural and functional methods we revealed that the utilized nanomicelles can positively affect root length, without any negative effects on leaf anatomy and photosynthetic efficiency at 0.2 g L^{-1}, while strong negative effects were recorded for 10 and 30 g(SPM) L^{-1} concerning root length, leaf histology, and photoprotection capability. Our data strongly suggest that SPM can safely be utilized for seed priming at specific concentrations and are suitable objects for further loading with plant growth regulators.

Keywords: chlorophyll fluorescence; garden pea; leaf anatomy; nanoparticles; plant biometry; poloxamer.

Introduction

Pluronics are synthetic triblock poly(ethylene oxide)-poly(propylene oxide)-poly(ethylene oxide) copolymers, where the poly(ethylene oxide) (PEO) blocks exhibit hydrophilic properties, while the poly(propylene oxide) (PPO) block is hydrophobic. Their amphiphilic character leads to the formation of micellar structures in an aqueous environment, with the hydrophobic blocks forming a water-insoluble core, which potentially can be loaded with lipophilic molecules/drugs, while the hydrophilic blocks form the outer hydrated shell (Batrakova and Kabanov 2008).

Pluronics (also called poloxamers) are biocompatible polymers, that are widely available, stable, easily soluble, and able to penetrate cellular membranes, which results in

Highlights

- Stabilized *Pluronic P85* nanomicelles as a beneficial priming agent for pea seeds
- Nanomicelles at concentration of 0.2 g L^{-1} stimulate root elongation
- Nanomicelles at 10 and 30 g L^{-1} impair root length, leaf anatomy, and photoprotection

Received 5 June 2023
Accepted 4 September 2023
Published online 25 September 2023

[+]Corresponding author
e-mail: violet@bio21.bas.bg

Abbreviations: Chl – chlorophyll; F_v/F_m – maximum quantum yield of PSII determined in dark-adapted state; LMA – leaf dry mass per unit area; NBI – nitrogen balance index; NPQ – nonphotochemical quenching of chlorophyll *a* fluorescence; PETA – pentaerythritol tetraacrylate; PPO – poly(propylene oxide); q_L – fraction of open PSII reaction centers; SPM – stabilized *Pluronic P85* micelles; Φ_{NO} – quantum yield of other nonphotochemical losses; Φ_{NPQ} – quantum yield of the downregulatory nonphotochemical quenching; Φ_{PSII} – actual quantum efficiency of PSII photochemistry determined in light-adapted state.

Acknowledgments: The authors are thankful to the Bulgarian Science Fund, grant number KP-06-H36/8/13.12.2019, for the financial support. SK is grateful to Prof. Győző Garab for his mentorship, support, and collaboration.
Conflict of interest: The authors declare that they have no conflict of interest.

their vast application as safe drug carriers with site-specific and slow-release properties. The length of the individual blocks can moderate the specific physical characteristics and consequently the physiological function of the polymer (Ottenbrite and Javan 2005, reviewed in Yu *et al*. 2021, Nugraha *et al*. 2022).

Pluronics can exert their effects by interaction with lipid membranes and modification of their properties, in strong dependence on the lipid composition, as thoroughly demonstrated for liposomes (Johnsson *et al*. 1999, Zhirnov *et al*. 2005, Zhang *et al*. 2019). Their interaction with human cells is also well studied (reviewed in Jarak *et al*. 2020), however, little is known about plant cells. Nevertheless, there are reports demonstrating that at specific experimental conditions, *Pluronic F-68* has growth-stimulating effects on protoplasts (Kumar *et al*. 1992, Lowe *et al*. 1995, Anthony *et al*. 1997), plant cell/tissue cultures (Kumar *et al*. 1992, Iordan-Costache *et al*. 1995, Khehra *et al*. 1995, Anthony *et al*. 1996, Cancino *et al*. 2001, Lee and Kim 2002, Kaparakis and Alderson 2003, Khatun *et al*. 2003, Kok *et al*. 2021), and microspore cultures (Barbulescu *et al*. 2011). The effect of *Pluronics* on intact plants of large crabgrass was studied by Nalewaja *et al*. (1998) who showed that *Pluronic P85* was one of the most effective adjuvants tested (among five types of *Pluronic* polymers) for the reduction of nicosulfuron herbicide phytotoxicity.

Polymeric (both natural and synthetic) nanoparticles are already used in precision farming for controlled delivery of fertilizers, pesticides, and antibiotics (Hill *et al.* 2015, Xin *et al.* 2018, Pereira *et al*. 2019, Xin *et al.* 2020a,b). Also, their potential as plant growth regulators/stimulators is being investigated (Pereira *et al*. 2019, Xin 2020a,b; Vinzant *et al*. 2023). In particular, recent studies showed that newly synthesized polysuccinimide nanoparticles mitigate Cu stress in corn by enhancing seed germination and seedling growth (Xin *et al*. 2020c). An *et al*. (2020) showed that poly(acrylic acid)-coated cerium oxide nanoparticles priming of cotton seeds exert multiple effects on seeds and plant morphology, physiology, and biochemistry in conditions of salt stress. However, a major advantage of synthetic polymers comes from the fact that their properties (molar mass, functionality, hydrophilic/hydrophobic balance, aggregation behavior) can be controlled and thus modulated to achieve a specific aim by altering and/or functionalizing the polymeric unimers, furthermore, the nanoparticle's core might be loaded with desired cargos for targeted delivery.

To shine further light on the benefits of utilizing synthetic polymeric nanoparticles in agriculture, the present work examines, for the first time, the effect of pea seed priming with stabilized *Pluronic P85* micelles (SPM) on seed germination, plant growth, and functional and structural traits of the photosynthetic apparatus. Biometric, physiological, functional, and structural analyses reveal stimulating and inhibiting SPM concentrations and strongly suggest that those nanomicelles might further be used for the development of nanocarriers of plant growth regulators.

Materials and methods

Synthesis and characterization of stabilized polymeric micelles: In a typical run, 6 g of $PEO_{26}PPO_{40}PEO_{26}$ were dissolved in 300 mL of distilled water at 55°C. Next, the temperature was adjusted to 50°C, and 0.9 g of pentaerythritol tetraacrylate (PETA), dissolved in 6 mL of acetone, was added dropwise to the micellar solution under stirring. The system was purged with argon for 30 min and then, irradiation with a full spectrum UV–Vis light (*Dymax 5000-EC* UV-curing equipment with a 400-W metal halide flood lamp; dose rate = 5.7 J cm^{-2} min^{-1}) for 30 min was applied. The impurities and non-crosslinked copolymer were removed by ultrafiltration (regenerated cellulose membranes, MWCO 10 kDa), and SPMs were recovered by freeze drying (yield 53%). $PEO_{26}PPO_{40}PEO_{26}$ (*Pluronic P85*, donated by *BASF*, Germany) and PETA (*Sigma-Aldrich*, Germany) were used as received. In this study, SPMs were chosen due to their advantages in terms of structural stability. Unlike dynamic micelles, SPMs maintain their micellar integrity at rigorous conditions, such as dilution below the critical micellar concentration/temperature, the addition of organic solvents, and ultrasound treatment (Petrov *et al*. 2005). Therefore, they are expected to be stable in the conditions of seed coat penetration and consequent development of plant tissues.

Dynamic light scattering (DLS) method, using a *ZetasizerNanoBrook 90Plus Zeta* (Brookhaven, USA) instrument, equipped with a 35-mW red diode laser (λ = 640 nm), at a scattering angle of 90°, was used to determine the hydrodynamic diameter of SPMs. The DLS measurement determines the particle size by taking into account the way the particle diffuses in the measuring medium (*i.e.*, it considers particle size along with any surface-bound ions that might affect its diffusion). DLS technique is nondestructive and suitable for the characterization of monodisperse solutions. For a solution of spherical particles with monomodal size distribution (as in our case), the hydrodynamic diameter measured by DLS is a very close approximation of the actual physical size of the particle (Schärtl 2007). The DLS measurements revealed that the SPM used in this study had a monomodal particle size distribution (Fig. 1) and the calculated hydrodynamic diameter (D_h) was 37 ± 2 nm.

The ζ potential was calculated by the instrument software, adopting the Smoluchowski equation: $\zeta = 4\pi\eta\upsilon/\varepsilon$, where η is the solvent viscosity, υ is the electrophoretic mobility, and ε is the dielectric constant of the solvent. The ζ potential of the utilized SPM was determined to be –2.9 ± 0.3 mV (Fig. 1*B*).

Seeds priming: *Pisum sativum* (var. RAN-1) seeds (garden pea) were primed with SPM aqueous solutions with concentrations of 0.04, 0.2, 1, 5, 10, and 30 g L^{-1} or with distilled water (henceforth named hydro-primed or control samples) for 6 h, applying slow rotatory shaking. At the end of this period, the imbibition level was determined, relative to the initial seeds dry mass. For each variant, 100 seeds were soaked in 100 ml of distilled

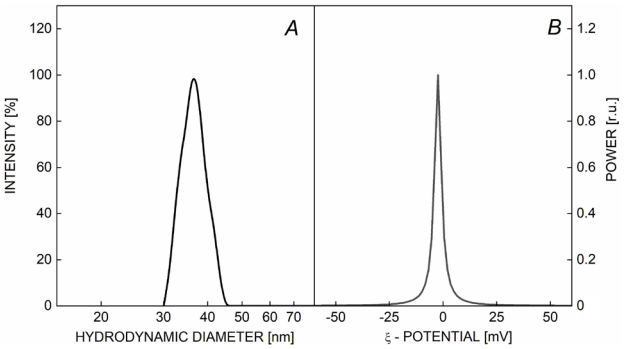

Fig. 1. Particle size distribution (*A*) and ζ-potential (*B*) plots of stabilized micelles based on $PEO_{26}PPO_{40}PEO_{26}$ triblock copolymer.

water or SPM solution. Next, the seeds were dried at room temperature and stored until further use. Before each experiment, the seeds were soaked in distilled water for 2 h and then were immediately placed on wet filter paper in the dark at 22°C ambient temperature and 65% air humidity, where they germinated for 4 d.

Seed germination and early plant development: Seed germinability (germination percentage) and synchrony of germination (it equals 1 when the germination of all seeds in different replications of specific treatment occurs at the same time and approaches 0 when their number decreases) were calculated as in Ranal *et al.* (2009). On the 4th d of seed germination, the root length was determined and the germinated seeds were transferred to hydroponic vessels filled with tap water and grown for additional 10 d (as in Krumova *et al.* 2023). At the end of this period, the following parameters were determined: percentage of developed plants, total dry biomass (TDB), vigor index, and leaf dry mass per unit area (LMA). Adaxial surface chlorophyll (Chl) and flavonoid abundance were measured by the *Dualex* instrument (*ForceA*, France). The nitrogen balance index (NBI) was determined from the Chl/flavonoids ratio.

Leaf anatomy: Anatomical characterization of detached leaves was performed by light microscopy as detailed in Velikova *et al.* (2020). *Nikon Eclipse 50i* (Tokyo, Japan) camera was used to capture images. A minimum of 30 transversal leaf sections from the 2nd and 3rd leaves were analyzed after fixation in 3% (m/v) glutaraldehyde (dissolved in 0.1 M sodium phosphate buffer, pH 7.4) for control and SPM variants. The representation of the spongy and the palisade parenchyma was calculated as a ratio to total mesophyll thickness expressed as percentage.

Chl fluorescence imaging: Chl fluorescence on intact leaves was performed on the 2nd and 3rd well-developed leaf pairs using *IMAGING-PAM* (*MAXI version*; *Walz GmbH*, Germany) supplemented with blue excitation light unit (*IMAG-MAX/L* LED) and *IMAG-K7* CCD camera on 30 min dark-adapted plants. The experimental design is presented in detail in Velikova *et al.* (2021). The maximum quantum yield of PSII determined in the dark-adapted state (F_v/F_m), the actual quantum efficiency of PSII photochemistry determined in the light-adapted state (Φ_{PSII}), nonphotochemical quenching of Chl *a* fluorescence (NPQ), the quantum yield of the downregulatory nonphotochemical quenching (Φ_{NPQ}), the quantum yield of other nonphotochemical losses (Φ_{NO}), and the fraction of open PSII reaction centers (q_L) were evaluated.

Statistical evaluation: Data shown represent the means ± SE. The sample size of each measurement is reported in the corresponding figure captions. For estimation of the statistical significance of the obtained results, one-way analysis of variance (*ANOVA*) was used followed by *Tukey*'s post hoc test at $P<0.05$. Before the tests, data were checked for normal distribution and homogeneity of variances. Significantly different means are shown by different letters. The software package *GraphPad InStat*, *ver. 3.10* for *Windows* was used (*GraphPad Software*, Boston, MA, USA).

Results

Seed germination and plant biometry: The parameters describing seed germination upon hydro- and SPM-priming are presented in Table 1. As can be seen, the mean values of seed imbibition and synchrony of germination determined for 0.2 g(SPM) L^{-1} were higher while for

Table 1. Germination of SPM-primed seeds. Imbibition values (expressed as % relative to initial seed dry mass) are estimated after 6 h of seeds incubation in SPM/water solution. Germinability [%] and synchrony of germination are evaluated on the fourth day of seed germination, as defined by Ranal *et al*. (2009). Mean values (± SE) are determined for 100 seeds. Data are subjected to one-way *ANOVA* followed by *Tukey*'s test. No significant differences between means are found at $P<0.05$.

SPM concentration [g L^{-1}]	Imbibition [%]	Germinability [%]	Synchrony of germination
0	86 ± 1	79 ± 5	0.68 ± 0.19
0.04	87 ± 4	84 ± 8	0.66 ± 0.18
0.2	87 ± 0.3	91 ± 5	0.70 ± 0.25
1	88 ± 2	88 ± 0	0.66 ± 0.17
5	82 ± 2	85 ± 7	0.63 ± 0.14
10	84 ± 4	79 ± 5	0.63 ± 0.19
30	79 ± 3	81 ± 1	0.58 ± 0.08

5–30 g L^{-1} variants tended to decrease, although the differences were not statistically significant. The average germinability was higher than the control for all SPM-primed variants, most pronounced for 0.2 g L^{-1} (by 15%) and 1 g L^{-1} (by 11%) SPM concentrations. However, the applied statistical analyses did not confirm the significant differences.

The next stages of plant development were evaluated based on root elongation on the 4th d after seed germination and on the biometric characteristics of 14-d-old seedlings. A clear increase in the root length (by 43%) was observed only for 0.2 g(SPM) L^{-1} (Fig. 2). The priming with a concentration range of 0.2–1 g(SPM) L^{-1} was associated with 11–15% increase in the mean relative number of developed plants, and 33% increase in the mean vigor index, respectively, as compared to plants developed from hydro-primed seeds. SPM priming at 10 g L^{-1} was related to a decrease in dry mass and vigor index by 25%, although the differences were not significant. The mean values of LMA also varied insignificantly in a narrow range (Fig. 2).

Leaf anatomy and physiology: Leaves of pea plants developed from primed seeds possessed typical anatomical structures for dicotyledons (Metcalfe and Chalk 1979). They were bifacial and amphistomatic with an average thickness of the lamina of 247 ± 10 µm (Table 2). The mesophyll was structured in single-rowed palisade parenchyma and multi-rowed spongy parenchyma with typical morphological characteristics of cells (Fig. 1S*A*,*B*; *supplement*). The palisade parenchyma consisted of upright, vertically oblong, and densely packed cells, while the spongy parenchyma, located above the lower epidermis, was loosely arranged and enclosed large intercellular spaces. Palisade and spongy parenchyma represented about 20 and 80% of the whole photosynthetic tissue, respectively. While the histological organization of the leaves was similar for all investigated SPM variants (Fig. 1S), at the cellular level, an effect of SPM seed priming was observed at 5 g(SPM) L^{-1} (Fig. 1S*C*,*D*), where the cells did not have the typical elongated cylindrical shape. The morphometric data revealed a clear tendency of

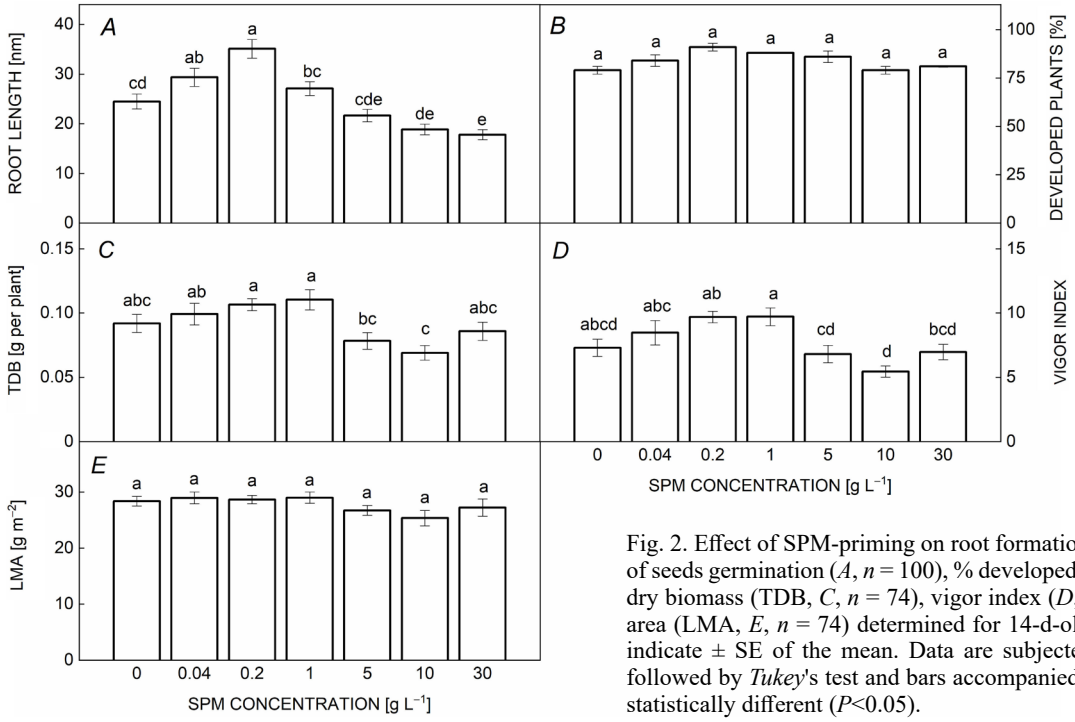

Fig. 2. Effect of SPM-priming on root formation estimated on the 4th d of seeds germination (*A*, *n* = 100), % developed plants (*B*, *n* = 90), total dry biomass (TDB, *C*, *n* = 74), vigor index (*D*, *n* = 74) and leaf mean area (LMA, *E*, *n* = 74) determined for 14-d-old seedlings. Error bars indicate ± SE of the mean. Data are subjected to one-way *ANOVA* followed by *Tukey*'s test and bars accompanied by *different letters* are statistically different (P<0.05).

Table 2. Anatomical traits of pea leaves developed from hydro-primed control seeds and seeds primed with different concentrations of SPM. Mean ± SE (*n* = 30). Data are subjected to one-way *ANOVA* followed by *Tukey*'s test. Means in the same column that are statistically different are shown by *different letters* (P<0.05).

SPM concentration [g L^{-1}]	Leaf thickness [µm]	Adaxial and abaxial epidermis thickness [µm]	Mesophyll thickness [µm]	Palisade parenchyma thickness [µm]	Spongy parenchyma thickness [µm]	Palisade coefficient
0	247 ± 10^{a}	39 ± 5^{a}	205 ± 15^{a}	43 ± 8^{a}	164 ± 10^{a}	21
5	225 ± 16^{a}	40 ± 6^{a}	183 ± 18^{ab}	34 ± 9^{a}	139 ± 13^{ab}	20
10	170 ± 17^{b}	33 ± 5^{a}	136 ± 15^{bc}	35 ± 7^{a}	106 ± 12^{bc}	25
30	112 ± 13^{c}	31 ± 6^{a}	90 ± 17^{c}	30 ± 8^{a}	64 ± 13^{c}	33

a decline in the average thickness of lamina as a response to the increasing concentrations of SPM. Indeed, seed priming with 10 and 30 g(SPM) L^{-1} reduced the lamina thickness by 30 and 55%, respectively, compared to hydro-primed samples (Table 2), and this was due to the reduction of spongy parenchyma. Histological analysis showed that the cells of the spongy parenchyma were more closely spaced and the apoplast was greatly reduced (Fig. 1S*C*,*E*,*G*). As a consequence of these changes, the coefficient of palisade increased from 21% in the control to 33% in 30 g(SPM) L^{-1}.

The adaxial leaf surface pigment measurements revealed that SPM priming in the applied concentration range did not alter the total Chl amount. The flavonoid content, however, significantly increased for 1 g(SPM) L^{-1}. The NBI parameter was largely reduced also for 1 g(SPM) L^{-1} concentration (Fig. 3).

Leaf photosynthetic efficiency: Chl fluorescence imaging on intact leaves was utilized to evaluate the photosynthetic efficiency alteration as a result of SPM seed priming. The values of maximal efficiency of PSII in the dark-adapted leaves were not significantly different between the studied variants. A statistically significant effect was observed for Φ_{PSII} after 30 g(SPM) L^{-1} application (an increase of 13%), and for q_L in 10–30 g(SPM) L^{-1} variants (an increase of 12–19%) in comparison with hydro-primed ones (Fig. 4).

The traces recorded for NPQ development for 15-min illumination revealed pronounced retardation of NPQ development for the initial 6 min for 0.04 and 10 g(SPM) L^{-1}, however, those variants were able to reach the control NPQ values at the end of the illumination period (Fig. 5). A significant reduction in NPQ parameter evaluated after 15 min of illumination with actinic light was detected only for 30 g(SPM) L^{-1} priming, by 18% (Fig. 5).

Finally, we evaluated the portion of light energy that is utilized for photochemistry (*i.e.*, photosynthesis) and the one dissipated in the process of nonphotochemical pathways (Φ_{NPQ} and Φ_{NO}). The analysis revealed that only 30 g(SPM) L^{-1} priming induced statistically significant

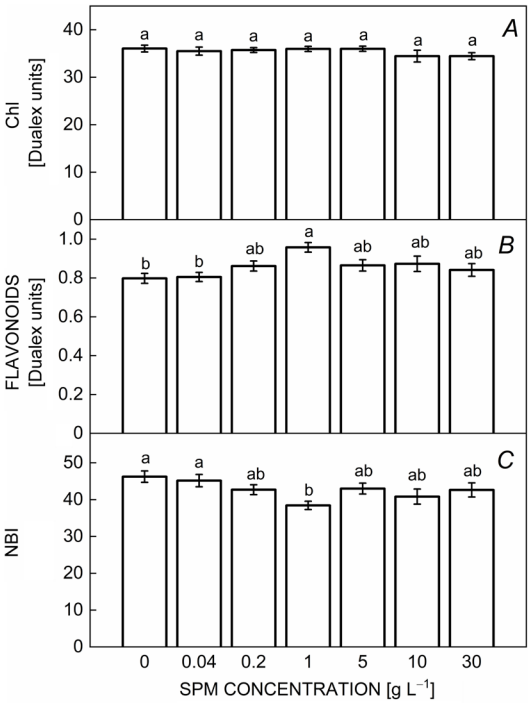

Fig. 3. Effect of SPM-priming on leaf pigments measured by *Dualex* instrument on intact 14-d-old seedlings: total chlorophyll content (Chl, *A*), total flavonoids content (*B*), nitrogen balance index (NBI, *C*). Mean ± SE (n = 25). Data are subjected to one-way *ANOVA* followed by *Tukey*'s test and bars accompanied by *different letters* are statistically different (P<0.05).

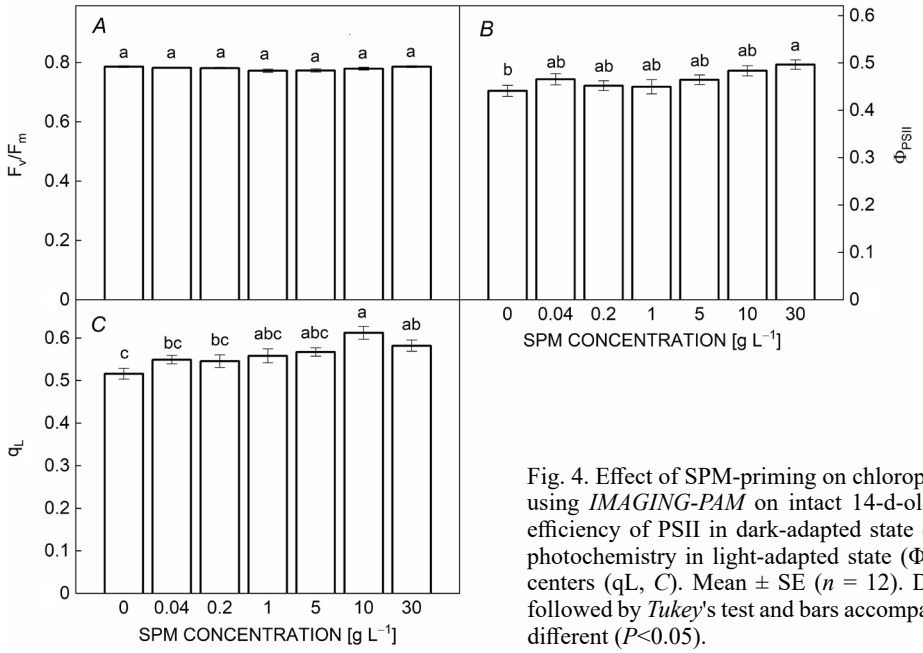

Fig. 4. Effect of SPM-priming on chlorophyll fluorescence parameters evaluated using *IMAGING-PAM* on intact 14-d-old seedlings: maximum photochemical efficiency of PSII in dark-adapted state (F_v/F_m, *A*), quantum efficiency of PSII photochemistry in light-adapted state (Φ_{PSII}, *B*), fraction of open PSII reaction centers (qL, *C*). Mean ± SE (n = 12). Data are subjected to one-way *ANOVA* followed by *Tukey*'s test and bars accompanied by *different letters* are statistically different (P<0.05).

changes in the light-energy utilization by pea plants, related to higher PSII and lower NPQ quantum yields. The values of Φ_{NO} for all variants were similar (Fig. 6).

Discussion

Nanoparticle utilization for the enhancement of seed germination and plant growth is not a new scientific and agronomical approach. There are many studies demonstrating the potential as well as the limitation (concerning soil pollution and phytotoxicity) of a large variety of nanoparticles for plant growth regulation (Szőllősi *et al*. 2020, Adhikari *et al*. 2021).

In the present work for the first time, we have evaluated the effect of pea seed priming with SPM composed of *Pluronic P85* polymer on germination, seedling development, leaf anatomy, and photochemical efficiency. We chose those nanoparticles as interesting study objects, since they are small and, thus, are expected to transverse plant cell walls and membranes, and can reach distant plant tissues. They are biocompatible (Jeong 2011, Almeida *et al*. 2018), and adjustable allowing for the loading of hydrophobic substances within their core and thus can serve as efficient nanocarriers. We have studied a large concentration range (0.04–30 g L^{-1}) since it is well-known that nanoparticles in general exhibit dual effects (stimulating/inhibiting) at different concentrations. This was demonstrated for *Pluronic F-68* which exhibits optimal effect at 1 g L^{-1} concerning callus growth, while concentrations above 10 g L^{-1} are inhibiting this process (Anthony *et al*. 1994). More recently, another work demonstrated that supplementation of 0.4 g L^{-1} *Pluronic F-68* induced enhancement of callus proliferation by stimulating various metabolic pathways, while 1 g L^{-1} induced stress response in the callus development (Kok *et al*. 2021). This indicates that SPM could be used as growth additives only at appropriate concentrations. It should, however, be noted that the effects of *Pluronic F-68* cannot be extrapolated to *Pluronic P85* used in this study due to the differences in their structure ($PEO_{76}PPO_{29}PEO_{76}$ for *F-68 vs*. $PEO_{26}PPO_{40}PEO_{26}$ for *P85*). *Pluronic F-68* is more hydrophilic while *Pluronic P85* is more lipophilic and thus it is expected to have a different mode of interaction with plants.

The results present in this work demonstrate: (*1*) stimulating effect at 0.2 g(SPM) L^{-1} concentration concerning root elongation, without any damaging effects on seeds germination, leaf anatomy, and photosynthetic performance; (*2*) inhibiting effect at 10–30 g(SPM) L^{-1} resulting in reduced root length, leaf spongy parenchyma, apoplast, and photoprotection capability. Since the apoplast structure is already determined in the embryo, genetic and metabolic factors during seed germination should be responsible for its alteration as a consequence of SPM seed priming. Spongy tissue has multiple functions, such as scattering and absorbing light, and facilitating CO_2 diffusion from the stomata to the palisade tissue (Smith *et al*. 1997, Terashima *et al*. 2011). It was demonstrated that structural organization and scaling of spongy parenchyma are associated with leaf function

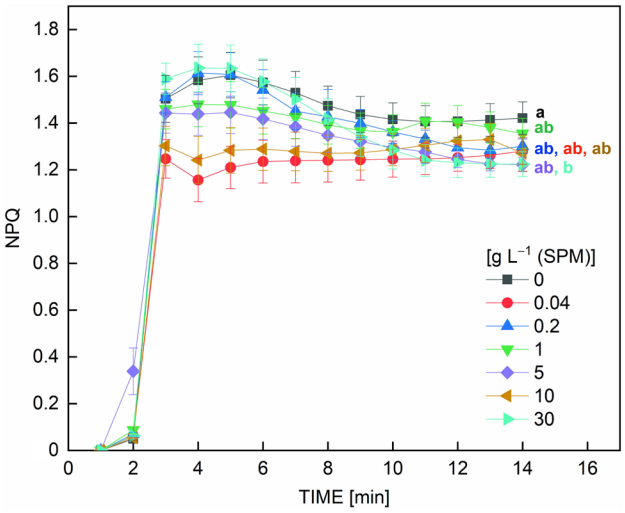

Fig. 5. Effect of SPM-priming on NPQ development evaluated using *IMAGING-PAM* on intact 14-d-old seedlings. The different SPM concentrations utilized for seed priming are indicated in the figure legend. Mean ± SE (n = 12). The last data points at 14th min are subjected to one-way *ANOVA* followed by *Tukey*'s test and *different letters* indicate statistically significant differences (P<0.05).

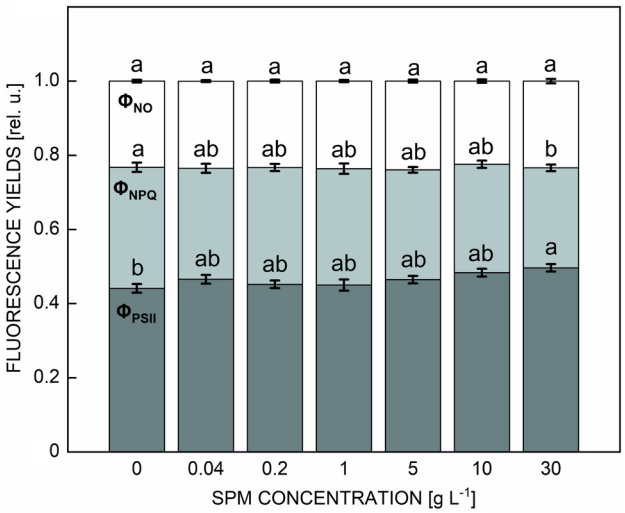

Fig. 6. Partitioning of a fraction of excitation energy flow *via* PSII photochemistry (Φ_{PSII}) and nonphotochemical dissipation pathways (Φ_{NPQ} and Φ_{NO}) determined using *IMAGING-PAM* on intact 14-d-old hydro- or SPM-primed seedlings. Mean ± SE (n = 12). Data are subjected to one-way *ANOVA* followed by *Tukey*'s test and bars accompanied by *different letters* are statistically different (P<0.05) only within the given dataset (excitation energy allocation parameters).

and cell arrangement and that intercellular airspaces are an important factor for proper leaf function (Borsuk *et al*. 2022). The reduced intercellular spaces in 10 g(SPM) L^{-1} may restrict carbon flow toward the chloroplasts, decreasing photosynthesis. Our data suggest that densely packed cells lead to a specific structural configuration of a spongy parenchyma that can negatively influence

mesophyll conductance to CO_2, which represents a major limitation factor on photosynthetic functioning (Lehmeier *et al*. 2017, Gago *et al*. 2020, Théroux-Rancourt *et al*. 2021). Our results strongly suggest that the plants developed from seeds primed with 10 and 30 g(SPM) L^{-1} try to compensate for the impaired functionality of PSII for photoprotection by increasing the number of PSII reaction centers (evaluated by q_L parameter) and thus the total effective PSII quantum yield (Φ_{PSII} parameter). Moreover, the Φ_{PSII} increased with a concurrent decrease of the Φ_{NPQ} as a part of the total thermal dissipation (Φ_{NPQ+NO}). These results indicate that seed priming with 10–30 g(SPM) L^{-1} reduced the photoprotective capability of the plants.

On the other hand, higher amount of flavonols is observed only in plants developed from seeds primed with 1 g(SPM) L^{-1}, indicating that they might be better prepared to meet various environmental stress stimuli (Brunetti *et al*. 2019). Further increase in SPM concentration (*i.e*., 30 g L^{-1}) during the priming procedure resulted in the most pronounced reduction of the spongy parenchyma, and no effect on other parameters analyzed (germination, biomass, photosynthetic efficiency) was found. This could be partially explained by the highest palisade coefficient in this variant among all other variants, which positively affects multiple aspects of plant development.

The question arises as to why bare SPM, which are not loaded or surface-modified with plant growth stimulator, would affect seedling development and if this effect is due to the direct interaction of SPM with root and leaves tissues/cells or is a consequence of altered metabolic processes occurring in the seeds during germination? The first barrier that SPM faces during the priming procedure is the seed coat – a largely impermeable structure, that however allows for water penetration upon a change in temperature and humidity of the surrounding environment, as well as upon mechanical stimuli, microbial contact, or animal gut passage. The mechanism by which it is achieved is intensively investigated but still unclear. Janská *et al*. (2019) have suggested that seed dormancy break in pea is associated with both changes in the lipid layer of the seed coat and its mechanical disruption. There are studies demonstrating that nanoparticles in general can penetrate cell walls even when their physical sizes overcome the actual pore size (for review *see* Kurczyńska *et al*. 2021). Furthermore, there are numerous reports evidencing the direct interaction of *Pluronics* with biological membranes that results in alteration in membrane microviscosity (Batrakova *et al*. 2001, Batrakova and Kabanov 2008) and lipid diffusion (Wang *et al*. 2014), resealing of injured membranes (Kwiatkowski *et al*. 2020), and alteration of functions of various transporters and other membrane proteins (Alakhova and Kabanov 2014). The contribution of apoplast and symplast in the uptake and movement of nanoparticles within the plant body is also comprehensively discussed (Kurczyńska *et al*. 2021). It appears likely that SPM enter the water flow in the phloem and xylem and thus interact with a variety of water-soluble substances and/or reach different plant tissues and membranes.

It should also be noted that the *Pluronics* aggregation behavior appears as a major factor that determines their interaction with seeds during the early stages of seed germination and seedling development. Our recent study characterized the effect of priming with *Pluronic P85* non-crosslinked micelles (applied in the same concentrations as in the current work) and demonstrated pronounced negative effects on seedlings biomass accumulation, survival, and capability for photoprotection (Krumova *et al*. 2023). Those *P85* micelles are dynamic aggregates, they are smaller (D_h ~ 20 nm) than SPM and can easily dissociate to unimers upon dilution. Their different physical properties, as compared to the SPM utilized in the present work, also ensure different interactions with seeds during the priming procedure and as a consequence different effects on plant development.

Despite the extensive research and a large amount of literature data collected, the topic of how plant–nanoparticles interact and what are the mechanisms that regulate this process still have many unanswered questions and require further in-depth studies.

Conclusions: Although the exact roles of *Pluronics* in seed tissues are not yet established, our results strongly suggest that SPM do penetrate seed coat, plant cell walls, and membranes and exert short-term (during germination) as well as long-lasting (at the time scale of our study) effects on plant growth and photosynthetic function. In particular, pea seed priming with SPM composed of *Pluronic P85* exerts a positive effect at 0.2 g L^{-1} and a negative effect at 10–30 g L^{-1} on early seedling development. The observed effects strongly suggest that the optimal concentration of 0.2 g(SPM) L^{-1} can be used for further development of *Pluronic P85* stabilized nanomicelles loaded with substances beneficial for plant growth and plant plasticity in terms of environmental stress adaptation.

References

Adhikari K., Mahato G.R., Chen H. *et al*.: Nanoparticles and their impacts on seed germination. – In: Singh V.P., Singh S., Tripathi D.K. *et al*. (ed.): Plant Responses to Nanomaterials. Nanotechnology in the Life Sciences. Pp. 21-31. Springer, Cham 2021.

Alakhova D.Y., Kabanov A.V.: Pluronics and MDR reversal: an update. – Mol. Pharm. **11**: 2566-2578, 2014.

Almeida M., Magalhães M., Veiga F., Figueiras A.: Poloxamers, poloxamines and polymeric micelles: Definition, structure and therapeutic applications in cancer. – J. Polym. Res. **25**: 31, 2018.

An J., Hu P., Li F. *et al*.: Emerging investigator series: molecular mechanisms of plant salinity stress tolerance improvement by seed priming with cerium oxide nanoparticles. – Environ. Sci.-Nano **7**: 2214-2228, 2020.

Anthony P., Davey M.R., Power J.B. *et al*.: Synergistic enhancement of protoplast growth by oxygenated perfluorocarbon and Pluronic F-68. – Plant Cell Rep. **13**: 251-255, 1994.

Anthony P., Jelodar N.B., Lowe K.C. *et al*.: Pluronic F-68 increases the post-thaw growth of cryopreserved plant cells. – Cryobiology **33**: 508-514, 1996.

Anthony P., Lowe K.C., Davey M.R., Power J.B.: Strategies for promoting division of cultured plant protoplast: synergistic effects of haemoglobin (Erythrogen) and Pluronic F-68. –

Plant Cell Rep. **17**: 13-16, 1997.
Barbulescu D.M., Burton W.A., Salisbury P.A.: Pluronic F-68: an answer for shoot regeneration recalcitrance in microspore-derived *Brassica napus* embryos. – In Vitro Cell. Dev.-Pl. **47**: 282-288, 2011.
Batrakova E.V., Kabanov A.V.: Pluronic block copolymers: Evolution of drug delivery concept from inert nanocarriers to biological response modifiers. – J. Control. Release **130**: 98-106, 2008.
Batrakova E.V., Li S., Vinogradov S.V. *et al.*: Mechanism of pluronic effect on P-glycoprotein efflux system in blood-brain barrier: contributions of energy depletion and membrane fluidization. – J. Pharmacol. Exp. Ther. **299**: 483-493, 2001.
Borsuk A.M., Roddy A.B., Théroux-Rancourt G., Brodersen C.R.: Structural organization of the spongy mesophyll. – New Phytol. **234**: 946-960, 2022.
Brunetti C., Sebastiani F., Tattini M.: Review: ABA, flavonols, and the evolvability of land plants. – Plant Sci. **280**: 448-454, 2019.
Cancino G.O., Gill M.I.S., Anthony P. *et al.*: Pluronic F-68 enhanced shoot regeneration in a potencially novel citrus rootstock. – Artif. Cell. Blood Sub. Biotechnol. **29**: 317-324, 2001.
Gago J., Daloso D.M., Carriquí M. *et al.*: Mesophyll conductance: the leaf corridors for photosynthesis. – Biochem. Soc. T. **48**: 429-439, 2020.
Hill M.R., MacKrell E.J., Forsthoefel C.P. *et al.*: Biodegradable and pH-responsive nanoparticles designed for site-specific delivery in agriculture. – Biomacromolecules **16**: 1276-1282, 2015.
Iordan-Costache M., Lowe K.C., Davey M.R., Power J.B.: Improved micropropagation of *Populus* spp. by Pluronic F-68. – Plant. Growth Regul. **17**: 233-239, 1995.
Janská A., Pecková E., Sczepaniak B. *et al.*: The role of the testa during the establishment of physical dormancy in the pea seed. – Ann. Bot.-London **123**: 815-829, 2019.
Jarak I., Varela C.L., da Silva E.T. *et al.*: Pluronic-based nanovehicles: Recent advances in anticancer therapeutic applications. – Eur. J. Med. Chem. **206**: 112526, 2020.
Jeong B.: Injectable biodegradable materials. – In: Vernon B. (ed.): Injectable Biomaterials. Pp. 323-337. Woodhead Publishing, Cambridge 2011.
Johnsson M., Silvander M., Karlsson G., Edwards K.: Effect of PEO-PPO-PEO triblock copolymers on structure and stability of phosphatidylcholine liposomes. – Langmuir **15**: 6314-6325, 1999.
Kaparakis G., Alderson P.G.: Enhancement of *in vitro* cell proliferation of pepper (*Capsicum annuum* L.) by Pluronic F-68, haemoglobin and arabinogalactan proteins. – J. Hortic. Sci. Biotech. **78**: 647-649, 2003.
Khatun A., Naher Z., Mahboob S. *et al.*: An efficient protocol for plant regeneration from the cotyledons of kenaf (*Hibiscus cannabinus* L.). – Biotechnology **2**: 86-93, 2003.
Khehra M., Lowe K.C., Davey M.R., Power J.B.: An improved micropropagation system for *Chrysanthemum* based on Pluronic F-68-supplemented media. – Plant Cell Tiss. Org. Cult. **41**: 87-90, 1995.
Kok A.D.-X., Mohd Yusoff N.F., Sekeli R. *et al.*: Pluronic F-68 improves callus proliferation of recalcitrant rice cultivar *via* enhanced carbon and nitrogen metabolism and nutrients uptake. – Front. Plant Sci. **12**: 667434, 2021.
Krumova S., Petrova A., Petrova N. *et al.*: Seed priming with single-walled carbon nanotubes grafted with Pluronic P85 preserves the functional and structural characteristics of pea plants. – Nanomaterials **13**: 1332, 2023.
Kumar V., Laouar M.R., Davey B.J. *et al.*: Pluronic F-68 stimulates growth of *Solanum dulcamara* in culture. – J. Exp. Bot. **43**: 487-493, 1992.
Kurczyńska E., Godel-Jędrychowska K., Sala K., Milewska-Hendel A.: Nanoparticles–plant interaction: What we know, where we are? – Appl. Sci. **11**: 5473, 2021.
Kwiatkowski T.A., Rose A.L., Jung R. *et al.*: Multiple poloxamers increase plasma membrane repair capacity in muscle and nonmuscle cells. – Am. J. Physiol.-Cell Physiol. **318**: C253-C262, 2020.
Lee S.-Y., Kim D.-I.: Stimulation of murine granulocite macrophage-colony stimulation factor production by Pluronic F-68 and polyethylene glycol in transgenic *Nicotiana tabacum* cell culture. – Biotechnol. Lett. **24**: 1779-1783, 2002.
Lehmeier C., Pajor R., Lundgren M.R. *et al.*: Cell density and airspace patterning in the leaf can be manipulated to increase leaf photosynthetic capacity. – Plant J. **92**: 981-994, 2017.
Lowe K.C., Anthony P., Davey M.R. *et al.*: Enhanced protoplast growth at the interface between oxygenated fluorocarbon liquid and aqueous culture medium supplemented with Pluronic F-68. – Artif. Cell. Blood Sub. Biotechnol. **23**: 417-422, 1995.
Metcalfe C.R., Chalk L.: Anatomy of Dicotyledons. Vol. I: Systematic Anatomy of Leaf and Stem, with a Brief History of the Subject. Pp. 288. Clarendon Press, Oxford 1979.
Nalewaja J.D., Praczyk T., Matysiak R.: Nitrogen fertilizer, oil, and surfactant adjuvants with nicosulfuron. – Weed Technol. **12**: 585-589, 1998.
Nugraha D.H., Anggadiredja K., Rachmawati H.: Mini-review of poloxamer as a biocompatible polymer for advanced drug delivery. – Braz. J. Pharm. Sci. **58**: e21125, 2022.
Ottenbrite R.M., Javan R.: Biological structures. – In: Bassani F., Liedl G.L., Wyder P. (ed.): Encyclopedia of Condensed Matter Physics. Pp. 99-108. Elsevier, Oxford 2005.
Pereira A.E.S., Oliveira H.C., Fraceto L.F.: Polymeric nanoparticles as an alternative for application of gibberellic acid in sustainable agriculture: a field study. – Sci. Rep.-UK **9**: 7135, 2019.
Petrov P., Bozukov M., Tsvetanov C.B.: Innovative approach for stabilizing poly(ethylene oxide)-*b*-poly(propylene oxide)-*b*-poly(ethylene oxide) micelles by forming nano-sized networks in the micelle. – J. Mater. Chem. **15**: 1481-1486, 2005.
Ranal M.A., de Santana D.G., Ferreira W.R., Mendes-Rodrigues C.: Calculating germination measurements and organizing spreadsheets. – Braz. J. Bot. **32**: 849-855, 2009.
Schärtl W.: Light Scattering from Polymer Solutions and Nanoparticle Dispersions. Pp. 191. Springer, Berlin-Heidelberg 2007.
Smith W.K., Vogelmann T.C., DeLucia E.H. *et al.*: Leaf form and photosynthesis: do leaf structure and orientation interact to regulate internal light and carbon dioxide? – BioScience **47**: 785-793, 1997.
Szőllősi R., Molnár Á., Kondak S., Kolbert Z.: Dual effect of nanomaterials on germination and seedling growth: stimulation vs. phytotoxicity. – Plants-Basel **9**: 1745, 2020.
Terashima I., Hanba Y.T., Tholen D. *et al.*: Leaf functional anatomy in relation to photosynthesis. – Plant Physiol. **155**: 108-116, 2011.
Théroux-Rancourt G., Roddy A.B., Earles J.M. *et al.*: Maximum CO_2 diffusion inside leaves is limited by the scaling of cell size and genome size. – Proc. R. Soc. B **288**: e20203145, 2021.
Velikova V., Arena C., Izzo L.G. *et al.*: Functional and structural leaf plasticity determine photosynthetic performances during drought stress and recovery in two *Platanus orientalis* populations from contrasting habitats. – Int. J. Mol. Sci. **21**:

3912, 2020.
Velikova V., Petrova N., Kovács L. *et al.*: Single-walled carbon nanotubes modify leaf micromorphology, chloroplast ultrastructure and photosynthetic activity of pea plants. – Int. J. Mol. Sci. **22**: 4878, 2021.
Vinzant K., Rashid M., Khodakovskaya M.V.: Advanced applications of sustainable and biological nano-polymers in agricultural production. – Front. Plant Sci. **13**: 1081165, 2023.
Wang J., Segatori L., Biswal S.L.: Probing the association of triblock copolymers with supported lipid membranes using microcantilevers. – Soft Matter **10**: 6417-6424, 2014.
Xin X., He Z., Hill M.R. *et al.*: Efficiency of biodegradable and pH-responsive polysuccinimide nanoparticles (PSI-NPs) as smart nanodelivery systems in grapefruit: *in vitro* cellular investigation. – Macromol. Biosci. **18**: e1800159, 2018.
Xin X., Judy J.D., Sumerlin B.B., He Z.: Nano-enabled agriculture: from nanoparticles to smart nanodelivery systems. – Environ. Chem. **17**: 413-425, 2020a.
Xin X., Zhao F., Rho J.Y. *et al.*: Use of polymeric nanoparticles to improve seed germination and plant growth under copper stress. – Sci. Total Environ. **745**: 141055, 2020c.
Xin X., Zhao F., Zhao H. *et al.*: Comparative assessment of polymeric and other nanoparticles impacts on soil microbial and biochemical properties. – Geoderma **367**: 114278, 2020b.
Yu J., Qiu H., Yin S. *et al.*: Polymeric drug delivery system based on pluronics for cancer treatment. – Molecules **26**: 3610, 2021.
Zhang W., Coughlin M.L., Metzger J.M. *et al.*: Influence of cholesterol and bilayer curvature on the interaction of PPO-PEO block copolymers with liposomes. – Langmuir **35**: 7231-7241, 2019.
Zhirnov A.E., Demina T.V., Krylova O.O. *et al.*: Lipid composition determines interaction of liposome membranes with Pluronic L61. – BBA-Biomembranes **1720**: 73-83, 2005.